

基于 2,4,6-吡啶三羧酸配体桥连的铁(II)/镍(II) 配位聚合物的水热合成及结构表征

彭梦侠* 陈梓云

(嘉应学院化学系, 梅州 514015)

摘要: 在水热反应条件下 $\text{FeCl}_2 \cdot 6\text{H}_2\text{O}$ 、2,4,6-吡啶三羧酸 (H_3pyta) 和 NaOH 反应合成了 1 种一维链状铁配位聚合物 $[\text{Fe}_3(\text{pyta})_2(\text{H}_2\text{O})_8]$ (**1**); 同样条件下 $\text{Ni}(\text{OAc})_2 \cdot 4\text{H}_2\text{O}$ 、2,4,6-吡啶三羧酸(H_3pyta)、 NaOH 和 4-氨基-3,5-二(4-吡啶基)-1,2,4-三氮唑(abpt)反应合成了 1 种二维网状镍配合物 $[\text{Ni}_3(\text{pyta})_2(\text{abpt})_2(\text{H}_2\text{O})_3] \cdot 2\text{H}_2\text{O}$ (**2**)。通过元素分析和红外光谱对这 2 个配位聚合物进行了表征。单晶结构表明: 配合物 **1** 的晶体属于单斜晶系, Cc 空间群; 配合物 **2** 的晶体属于单斜晶系, $P2_1/c$ 空间群。在配合物 **1** 中, pyta^{3-} 配体采取 μ_2 -和 μ_4 - pyta^{3-} 2 种桥连模式将 Fe 原子连成了沿 c 轴方向延伸的 Fe-pyta 链。而在配合物 **2** 中, pyta^{3-} 配体仅采取 μ_2 -桥连模式将 Ni 原子连成线型三核 $[\text{Ni}_3(\text{pyta})_2]$ 单元, 这些三核单元进一步通过 abpt 辅助配体桥连成二维 (4,4) 层状结构。

关键词: 配位聚合物; 水热反应; 2,4,6-吡啶三羧酸; 4-氨基-二(4-吡啶基)-1,2,4-三氮唑

中图分类号: O614.81+1

文献标识码: A

文章编号: 1001-4861(2009)06-1055-07

Hydrothermal Synthesis and Crystal Structure of Fe(II)/Ni(II) Coordination Polymers Bridged by Pyridine-2,4,6-tricarboxylate

PENG Meng-Xia* CHEN Zi-Yun

(Department of Chemistry, Jiaying University, Meizhou, Guangdong 514015)

Abstract: Reaction of $\text{FeCl}_2 \cdot 6\text{H}_2\text{O}/\text{Ni}(\text{OAc})_2 \cdot 4\text{H}_2\text{O}$, pyridine-2,4,6-tricarboxylic acid (H_3pyta), NaOH results in formation of a 1D Fe-pyta chain based coordination polymer $[\text{Fe}_3(\text{pyta})_2(\text{H}_2\text{O})_8]$ (**1**), and another 2D coordination network $[\text{Ni}_3(\text{pyta})_2(\text{abpt})_2(\text{H}_2\text{O})_3] \cdot 3\text{H}_2\text{O}$ (**2**) with the auxiliary ligand 4-amino-3,5-bis(4-pyridyl)-1,2,4-triazole (abpt), both were characterized by elemental analysis and IR. X-ray diffraction crystal structure analysis shows that **1** crystallizes in monoclinic system, non-centrosymmetric space group Cc with $a=1.970\,2(3)$ nm, $b=0.682\,02(9)$ nm, $c=1.948\,1(2)$ nm, $\beta=117.063(2)^\circ$, $V=2.331\,1(5)$ nm³, $Z=8$; and **2** crystallizes in monoclinic system, space group $P2_1/c$ with $a=1.785\,19(18)$ nm, $b=0.725\,14(8)$ nm, $c=2.072\,5(2)$ nm, $\beta=112.574(2)^\circ$, $V=2.477\,3(4)$ nm³, $Z=4$. In complex **1**, the Fe atoms are connected by μ_2 - and μ_4 - pyta^{3-} ligands to form a 1D Fe-pyta chain with rhombic cores along the c -axis. While in complex **2**, the pyta^{3-} ligands adopt μ_2 -bridging mode to link the Ni atoms to linear trinuclear $[\text{Ni}_3(\text{pyta})_2]$ units, which are further connected to form 2D (4,4) coordination players by the auxiliary bridging ligand abpt. CCDC: 665831, **1**; 709969, **2**.

Key words: coordination polymer; hydrothermal reaction; pyridine-2,4,6-tricarboxylic acid; 4-amino-3,5-bis(4-pyridyl)-1,2,4-triazole

收稿日期: 2008-12-22。收修改稿日期: 2009-03-31。

广东省科技厅计划项目(No.2006B36703005)资助。

*通讯联系人。E-mail: pengmx123@sina.com

第一作者: 彭梦侠, 女, 44 岁, 硕士, 教授, 研究方向: 配位化学。

The design and synthesis of metal-organic coordination polymers are of great interest due to their novel structural topologies examined and potential applications in host-guest chemistry, catalysis, and electrical conductivity^[1-3]. In the rational design and synthesis of metal-organic coordination compounds, several factors are always taken into considerations, such as the coordination nature of metal ions, the functionality, flexibility and symmetry of organic ligands, and the template effect of structure-directing agents^[4-6]. 3- and 4-pyridinecarboxylate and pyridinedicarboxylate have recently been found to act as excellent building blocks with charge and multi-connecting ability in the construction of functional coordination polymers with porosity, photoluminescent or magnetic properties^[7,8]. Compared with the previously investigated pyridinecarboxylate ligands, pyridine-2,4,6-tricarboxylic acid ($H_3\text{pyta}$) have the advantages of multiple bridging moieties, which leads to a variety of connection modes with transition metal centers and provides abundant structural motifs. It can act not only as *N*-donors but also as $O_{\text{carboxylate}}$ -donors to chelate or bridge metal ions to coordination polymers^[9,10]. In our recent work, pyridine-2,4,6-tricarboxylic acid ($H_3\text{pyta}$) with 3d-4f metal ions have been used to construct coordination polymers with magnetic property or adsorption behavior^[11,12]. In this contribution, $H_3\text{pyta}$ was employed to synthesize a 1D Fe-pyta chain based coordination polymers $[\text{Fe}_3(\text{pyta})_2(\text{H}_2\text{O})_8]$ (**1**).

As is well known, the 4-amino-3,5-bis(4-pyridyl)-1,2,4-triazole (abpt) can be a good *N,N'*-donor building block that have been studied in coordination chemistry^[13-15]. As our continuous study of pyridine-2,4,6-tricarboxylate coordination polymers^[16,17], in this contribution, $H_3\text{pyta}$ was employed to synthesize a new 1D Fe-pyta chains based coordination polymer $[\text{Fe}_3(\text{pyta})_2(\text{H}_2\text{O})_8]$ (**1**); and another 2D coordination network $[\text{Ni}_3(\text{pyta})_2(\text{abpt})_2(\text{H}_2\text{O})_3] \cdot 3\text{H}_2\text{O}$ (**2**) constructed by $[\text{Ni}_3(\text{pyta})_2]$ units and the bridging 4-amino-3,5-bis(4-pyridyl)-1,2,4-triazole (abpt) ligands.

1 Experimental Section

1.1 Materials and physical measurements

The $\text{FeCl}_2 \cdot 6\text{H}_2\text{O}$ and $\text{Ni}(\text{OAc})_2 \cdot 4\text{H}_2\text{O}$ were comm-

ercially available and used as received without further purification. Pyridine-2,4,6-tricarboxylic acid ($H_3\text{pyta}$) was synthesized according to their literature methods^[18]. 4-amino-3,5-bis(4-pyridyl)-1,2,4-triazole (abpt) ligand could be obtained directly from the two reactants by employing the one-pot procedure described by Lagrenée and co-workers^[19]. The C, H and N microanalyses were carried out with an Elementar Vario-EL CHN elemental analyzer. The IR spectra were recorded from KBr tablets in the range $4000\sim 400\text{ cm}^{-1}$ on a Bio-Rad FTS-7 spectrometer.

1.2 Hydrothermal synthesis

$[\text{Fe}_3(\text{pyta})_2(\text{H}_2\text{O})_8]$ (**1**), A mixture of $\text{FeCl}_2 \cdot 6\text{H}_2\text{O}$ (352 mg, 1.5 mmol), $H_3\text{pyta}$ (211 mg, 1 mmol), NaOH (120 mg, 3 mmol) and H_2O (10 mL) was sealed in a 23 mL Teflon-lined reactor and heated in an oven at $185\text{ }^\circ\text{C}$ for 72 hrs and then at $90\text{ }^\circ\text{C}$ for 12 hrs. After 15 hrs' gradual cooling to room temperature, black-red crystals of **1** (yield 51% based on $H_3\text{pyta}$) were obtained, and then filtered, washed, and dried in air. Anal. Calcd. for $\text{C}_{16}\text{H}_{20}\text{Fe}_3\text{N}_2\text{O}_{20}$ (%): C, 26.40; H, 2.77; N, 3.85. Found (%): C, 26.29; H, 2.82; N, 3.92. IR (KBr, cm^{-1}): 3 420 (s), 1 577(vs), 1 408(m), 1 019(w), 923(w), 650(m).

$[\text{Ni}_3(\text{pyta})_2(\text{abpt})_2(\text{H}_2\text{O})_3] \cdot 2\text{H}_2\text{O}$ (**2**), A mixture of $\text{Ni}(\text{OAc})_2 \cdot 4\text{H}_2\text{O}$ (249 mg, 1 mmol), abpt (117 mg, 0.5 mmol), $H_3\text{pyta}$ (106 mg, 0.5 mmol), NaOH (20 mg, 0.5 mmol) and H_2O (10 mL) was sealed in a 23 mL Teflon-lined reactor and heated in an oven at $185\text{ }^\circ\text{C}$ for 72 hrs and then at $90\text{ }^\circ\text{C}$ for 12 hrs period. After 15 hrs' gradual cooling to room temperature, green crystals of **2** (yield 64% based on $H_3\text{pyta}$) were obtained, and then filtered, washed, and dried in air. Anal. Calcd. for $\text{C}_{40}\text{H}_{48}\text{N}_{14}\text{Ni}_3\text{O}_{24}$ (%): C, 37.39; H, 3.77; N, 15.26. Found (%): C, 37.47; H, 3.82; N, 15.15. IR (KBr, cm^{-1}): 3 653 (w), 3 358 (s), 1 634 (s), 1 562 (m), 1 474 (w), 1 436(m), 1 365(s), 1 316(m), 1 276(m), 1 217(w), 1 086(vw), 990 (vw), 931(vw), 842(m), 785(m), 743(s), 619(w), 540(w).

1.3 Crystal structure determination

Data collection of **1** and **2** was performed on a Bruker Smart Apex 1000 CCD diffractometer with Mo $K\alpha$ radiation ($\lambda=0.071\,073\text{ nm}$) at $293(2)\text{ K}$. The raw data frames were integrated with SAINT⁺, and the corrections were applied for Lorentz and polarization

effects. Absorption correction was applied by using the program SADABS^[20]. The structures were solved by direct methods, and all non-hydrogen atoms were refined anisotropically by least-squares on F^2 using the SHELXTL program^[21]. Hydrogen atoms on organic ligands were generated by the riding mode (C-H=0.093

nm). Crystal data as well as details of data collection and refinements for complexes **1** and **2** are summarized in Table 1. Selected bond distances and bond angles are listed in Table 2.

CCDC: 665831, **1**; 709969, **2**.

Table 1 Crystal data and structure parameters for complexes **1** and **2**

Identification code	1	2
Empirical formula	C ₁₆ H ₂₀ Fe ₃ N ₂ O ₂₀	C ₄₀ H ₄₈ N ₁₄ Ni ₃ O ₂₄
Formula weight	727.89	1 285.05
Temperature / K	293(2)	293(2)
Wavelength	0.710 73	0.710 73
Crystal system	Monoclinic	Monoclinic
Space group	<i>Cc</i>	<i>P2₁/c</i>
<i>a</i> / nm	1.970 2(3)	1.785 19(18)
<i>b</i> / nm	0.682 02(9)	0.725 14(8)
<i>c</i> / nm	1.948 1(2)	2.072 5(2)
β / (°)	117.063(2)	112.574(2)
Volume / nm ³	2.331 1(5)	2.477 3(4)
<i>Z</i>	4	2
<i>D_c</i> / (g·cm ⁻³)	2.074	1.723
Absorption coefficient / mm ⁻¹	1.949	1.232
<i>F</i> (000)	1 472	1 324
Crystal size / mm	0.26×0.21×0.19	0.16×0.10×0.08
θ range for data collection / (°)	2.35~26.00	3.01~26.00
Limiting indices	$-24 \leq h \leq 24, -8 \leq k \leq 8, -23 \leq l \leq 17$	$-20 \leq h \leq 20, -8 \leq k \leq 5, -22 \leq l \leq 25$
Reflections collected	5 665	9 424
Independent reflections (<i>R_{int}</i>)	3 420 (0.044 9)	4 693 (0.042 6)
Observed reflections [<i>I</i> >2 σ (<i>I</i>)]	3 235	3 354
Completeness / %	99.5	96.6
Refinement method	Full-matrix least-squares on F^2	Full-matrix least-squares on F^2
Data / restraints / parameters	3 420 / 12 / 370	4 693 / 20 / 415
Goodness-of-fit on F^2	1.013	0.911
Final <i>R</i> indices [<i>I</i> >2 σ (<i>I</i>)] <i>R</i> ₁ ^a , <i>wR</i> ₂ ^b	0.040 3, 0.096 7	0.042 2, 0.086 0
<i>R</i> indices (all data) <i>R</i> ₁ ^a , <i>wR</i> ₂ ^b	0.042 1, 0.097 9	0.060 2, 0.091 5
Largest diff. peak and hole	1.559, -0.658	0.609, -0.321

$$^a R_1 = \sum ||F_o| - |F_c|| / \sum |F_o|, ^b wR_2 = [\sum w(F_o^2 - F_c^2)^2 / \sum w(F_o^2)]^{1/2}.$$

Table 2 Bond lengths (nm) and angles (°) for **1** and **2**

1					
Fe(1)-O(8a)	0.209 0(4)	Fe(2)-O(4a)	0.207 5(4)	Fe(3)-O(5)	0.206 0(4)
Fe(1)-N(1)	0.210 3(4)	Fe(2)-O(5W)	0.210 0(4)	Fe(3)-O(7W)	0.210 1(5)
Fe(1)-O(1W)	0.212 3(4)	Fe(2)-O(4W)	0.212 1(4)	Fe(3)-N(2)	0.214 3(5)
Fe(1)-O(2W)	0.214 3(4)	Fe(2)-O(6W)	0.213 4(4)	Fe(3)-O(8W)	0.217 8(4)
Fe(1)-O(1)	0.216 6(4)	Fe(2)-O(2)	0.213 9(4)	Fe(3)-O(12)	0.219 6(4)
Fe(1)-O(6)	0.222 5(5)	Fe(2)-O(3W)	0.216 9(5)	Fe(3)-O(7)	0.222 3(6)

Continued Table 2

O(8a)-Fe(1)-N(1)	157.4(2)	O(4a)-Fe(2)-O(5W)	85.11(18)	O(5)-Fe(3)-O(7W)	81.20(17)
O(8a)-Fe(1)-O(1W)	83.65(17)	O(4a)-Fe(2)-O(4W)	104.01(16)	O(5)-Fe(3)-N(2)	171.57(18)
N(1)-Fe(1)-O(1W)	98.53(17)	O(5W)-Fe(2)-O(4W)	90.05(18)	O(7W)-Fe(3)-N(2)	100.57(18)
O(8a)-Fe(1)-O(2W)	87.29(17)	O(4a)-Fe(2)-O(6W)	86.41(18)	O(5)-Fe(3)-O(8W)	86.69(16)
N(1)-Fe(1)-O(2W)	91.90(16)	O(5W)-Fe(2)-O(6W)	99.54(18)	O(7W)-Fe(3)-O(8W)	167.83(18)
O(1W)-Fe(1)-O(2W)	169.46(16)	O(4W)-Fe(2)-O(6W)	166.48(18)	N(2)-Fe(3)-O(8W)	91.24(17)
O(8a)-Fe(1)-O(1)	128.4(2)	O(4a)-Fe(2)-O(2)	163.21(15)	O(5)-Fe(3)-O(12)	99.03(16)
N(1)-Fe(1)-O(1)	74.19(16)	O(5W)-Fe(2)-O(2)	86.37(16)	O(7W)-Fe(3)-O(12)	97.2(2)
O(1W)-Fe(1)-O(1)	89.65(17)	O(4W)-Fe(2)-O(2)	90.43(15)	N(2)-Fe(3)-O(12)	72.60(17)
O(2W)-Fe(1)-O(1)	91.80(17)	O(6W)-Fe(2)-O(2)	80.77(17)	O(8W)-Fe(3)-O(12)	83.41(17)
O(8a)-Fe(1)-O(6)	84.7(2)	O(4a)-Fe(2)-O(3W)	95.13(18)	O(5)-Fe(3)-O(7)	116.65(18)
N(1)-Fe(1)-O(6)	72.63(17)	O(5W)-Fe(2)-O(3W)	174.84(19)	O(7W)-Fe(3)-O(7)	82.9(2)
O(1W)-Fe(1)-O(6)	96.19(18)	O(4W)-Fe(2)-O(3W)	84.89(18)	N(2)-Fe(3)-O(7)	71.78(19)
O(2W)-Fe(1)-O(6)	88.28(17)	O(6W)-Fe(2)-O(3W)	85.61(19)	O(8W)-Fe(3)-O(7)	103.86(19)
O(1)-Fe(1)-O(6)	146.81(15)	O(2)-Fe(2)-O(3W)	94.66(17)	O(12)-Fe(3)-O(7)	143.75(19)
2					
Ni(1)-N(1)	0.197 4(2)	Ni(1)-O(2W)	0.207 7(3)	Ni(2)-O(1Wb)	0.208 7(2)
Ni(1)-N(7a)	0.204 3(3)	Ni(1)-O(2)	0.214 9(2)	Ni(2)-O(1W)	0.208 7(2)
Ni(1)-O(3W)	0.206 5(3)	Ni(2)-O(6b)	0.206 4(2)	Ni(2)-N(6b)	0.209 3(3)
Ni(1)-O(5)	0.207 7(2)	Ni(2)-O(6)	0.206 4(2)	Ni(2)-N(6)	0.209 3(3)
N(1)-Ni(1)-N(7a)	176.60(11)	N(1)-Ni(1)-O(2)	77.42(10)	O(1Wb)-Ni(2)-O(1W)	180.0
N(1)-Ni(1)-O(3W)	95.21(11)	N(7a)-Ni(1)-O(2)	105.23(10)	O(6b)-Ni(2)-N(6b)	85.91(9)
N(7a)-Ni(1)-O(3W)	86.75(11)	O(3W)-Ni(1)-O(2)	94.42(12)	O(6)-Ni(2)-N(6b)	94.09(9)
N(1)-Ni(1)-O(5)	78.75(9)	O(5)-Ni(1)-O(2)	156.12(8)	O(1Wb)-Ni(2)-N(6b)	89.43(10)
N(7a)-Ni(1)-O(5)	98.64(10)	O(2W)-Ni(1)-O(2)	85.98(11)	O(1W)-Ni(2)-N(6b)	90.57(10)
O(3W)-Ni(1)-O(5)	86.30(11)	O(6b)-Ni(2)-O(6)	180.00(13)	O(6b)-Ni(2)-N(6)	94.09(9)
N(1)-Ni(1)-O(2W)	89.41(12)	O(6b)-Ni(2)-O(1Wb)	87.70(10)	O(6)-Ni(2)-N(6)	85.91(9)
N(7a)-Ni(1)-O(2W)	88.66(12)	O(6)-Ni(2)-O(1Wb)	92.30(10)	O(1Wb)-Ni(2)-N(6)	90.57(10)
O(3W)-Ni(1)-O(2W)	175.34(12)	O(6b)-Ni(2)-O(1W)	92.30(10)	O(1W)-Ni(2)-N(6)	89.43(10)
O(5)-Ni(1)-O(2W)	95.21(11)	O(6)-Ni(2)-O(1W)	87.70(10)	N(6b)-Ni(2)-N(6)	180.0

Symmetry codes for **1**: (a) $x+1/2, -y+1/2, z+1/2$; (b) $x-1/2, -y+1/2, z-1/2$; for **2**: (a) $x-1, -y-5/2, z-1/2$; (b) $-x-1, -y-3, -z$.

2 Results and discussion

2.1 Synthesis

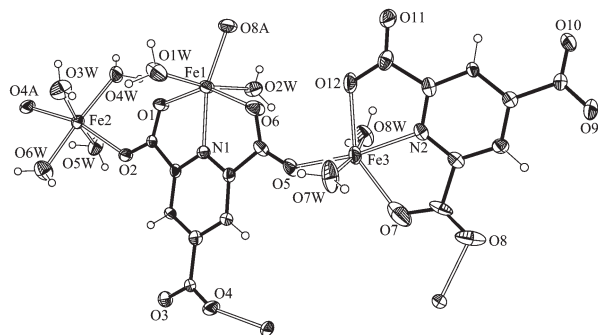
As is well known, there are a variety of hydrothermal parameters such as time, temperature, pH value, and molar ratio of reactants, and small changes in one or more of the parameters can have a profound influence on the final reaction outcome^[22]. In our previous work, we have reported a 1D Fe-pyta chain based coordination polymers $[\text{Fe}(\text{Hpyta})(\text{H}_2\text{O})_2]^{[16]}$,

obtained by the reaction of $\text{FeCl}_2 \cdot 6\text{H}_2\text{O}$, H_3pyta and NaOH in the molar ratio of 1:1:3 in the hydrothermal system at 185 °C. Considering the various connection modes of pyta ligand, we increased the molar ratio to 1.5:1:3, resulting the complex **1** based on Fe-pyta ladder-like chains with both μ_4 -pyta and μ_2 -pyta bridging ligands. Differently, there was no crystals obtained when the similar reaction reacted with Ni(II) ions. However, when the auxiliary ligand abpt was employed into the reaction system, complex **2** was

obtained, which was a 2D coordination polymer constructed by $[\text{Ni}_3(\text{pyta})_2]$ units and the bridging abpt, compared to the $(\text{H}_2\text{bpt})[\text{Fe}(\text{pyta})(\text{H}_2\text{O})_2] \cdot 4\text{H}_2\text{O}$ (H_2bpt =protonated 3,5-bis(4-pyridyl)-4H-1,2,4-triazol)^[14].

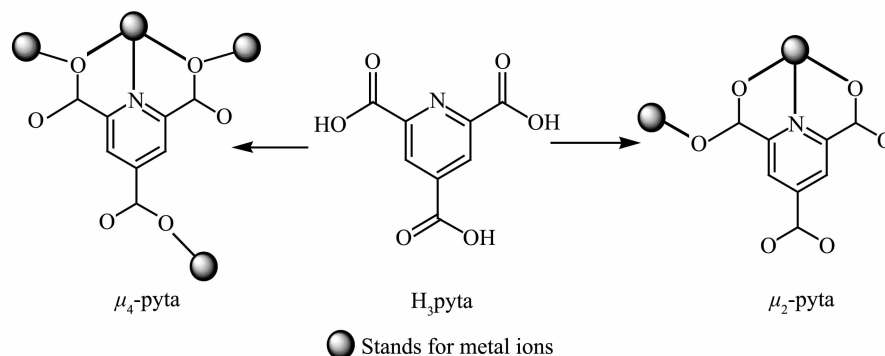
2.2 Structure of $[\text{Fe}_3(\text{pyta})_2(\text{H}_2\text{O})_8]$ (**1**)

Single crystal structure shows that complex **1** crystallizes in the monoclinic non-centrosymmetric space group Cc , with containing three crystallographically unique Fe(II) atoms, two deprotonated pyta³⁻ ligand and eight coordinated water molecules, all of which are on general positions (Fig.1). All of the three Fe(II) atoms adopt greatly distorted octahedral coordination geometry: Fe1 and Fe3 are similarly coordinated to three O atoms and one N atom from the pyta³⁻ ligand and two water molecules (Fe1-O=0.209 1(5)~0.222 4(5) nm; Fe1-N=0.210 3(4) nm; O-Fe1-O=83.62(17)°~169.39(17)°; O-Fe1-N=72.63(17)°~157.4(2)° (Fe3-O=0.206 0(5)~0.222 5(7) nm; Fe3-N=0.214 3(5) nm; O-Fe3-O=81.15(19)°~167.8(2)°; O-Fe3-N=71.8(2)°~171.54(18)°), while Fe2 is coordinated to two O atoms from the pyta³⁻ ligand and four water molecules (Fe2-



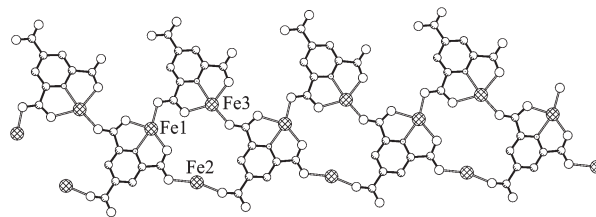
A: $x+1/2, -y+1/2, z+1/2$; B: $x-1/2, -y+1/2, z-1/2$

Fig.1 Coordination environment of Fe(II) atoms and coordination modes of pyta ligand in a asymmetric unit of **1**



Scheme 1 Coordination modes of pyta in complex **1** and **2**

O=0.207 5(4)~0.214 0(4) nm; O-Fe2-O=85.17(19)°~166.5(2)°). There are two coordination modes of the pyta³⁻ ligand, one of which adopts μ_4 -bridged mode connecting to four metal atoms and the other adopts μ_2 -bridged mode (Scheme 1). Interestingly, three metal atoms and three pyta³⁻ ligand (two μ_4 -bridged and one μ_2 -bridged) form a distorted rhombic core, each of which is stringed by the shared μ_4 -bridged pyta³⁻ ligand into the Fe-pyta chain along the c-axis (Fig.2). These cores are filled with the coordinated water molecules. Adjacent chains are packed in offset face-to-face AB method (Fig.3) through π - π interactions between the two pyridyl planes with the distance of 0.36 nm and rich hydrogen-bonds (O...O=0.272 2~0.289 2 nm, O-



Water molecules are omitted for clarity

Fig.2 Perspective view of the Fe-pyta ladder-like chain along the c-axis of **1**

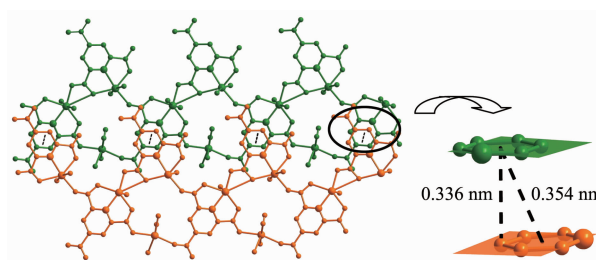


Fig.3 Perspective view of the Fe-pyta chains packed in offset face-to-face AB method through π - π interactions (the distances of the two pyridyl planes 0.336 nm and the two centers 0.354 nm) of **1**

HO = 150.39° ~ 167.29°) (Fig.4) between the water molecules and the carboxylate groups to generate a 3D supramolecular structure.

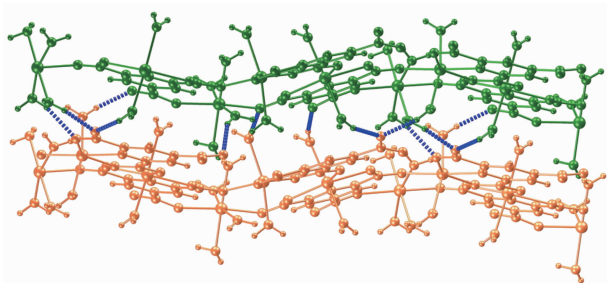


Fig.4 Perspective view of the hydrogen-bonds between the water molecules and the carboxylate groups of the adjacent packed Fe-pyta chains of **1**

2.3 Structure of $[\text{Ni}_3(\text{pyta})_2(\text{abpt})_2(\text{H}_2\text{O})_3] \cdot 3\text{H}_2\text{O}$ (**2**)

The crystal structure reveals that complex **2** is a 2D coordination polymer based on trinuclear $[\text{Ni}_3(\text{pyta})_2]$ units by the bridging abpt ligands. There are two unique Ni(II) atoms, one of which lies on special position, one deprotonated pyta³⁻ ligand, three coordinated and three lattice water molecules in the asymmetric unit (Fig.5). Ni1 has six-coordinate octahedral coordination environment with two O atoms and two N atom from the carboxylate group and pyridyl ring of the pyta³⁻ ligands and abpt ligand (Ni1-O=0.207 7(2) and 0.214 9(2) nm; Ni1-N=0.197 4(2) and 0.204 3(3) nm; O-Ni1-O=156.12(8)°; O-Ni1-N=77.42(10)°~105.23(10)°; N-Ni1-N=176.60(11)°) at basal positions and two water molecules at the apical positions (Ni1-O1W=0.206 5(3) and 0.207 7(3) nm; O1W-Ni1-O1W=175.34(12)°; O1W-Ni1-N/O=86.75(11)°~94.42(12)°). Ni2 atom, which lies on special position, also adopts hexagonal octahedral coordination geometry with two O atoms and two N atom from the carboxylate

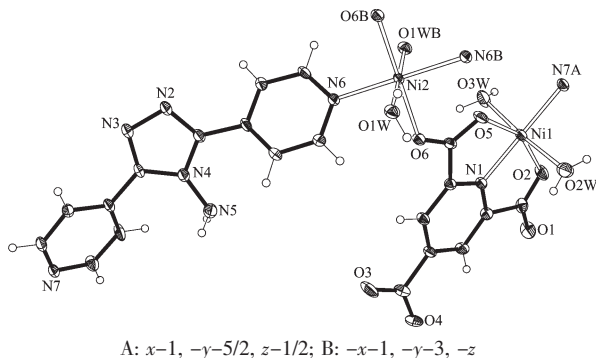


Fig.5 Coordination environment of Ni atoms in the asymmetric unit of **2**

group and pyridyl ring of the pyta³⁻ ligands (Ni2-O=0.207 7(2) and 0.214 9(2) nm; Ni2-N=0.197 4(2) and 0.204 3(3) nm; O-Ni2-O=156.12(8)°; O-Ni2-N=77.42(10)°~105.23(10)°; N-Ni2-N=176.60(11)°) at basal positions and two water molecules at the apical positions (Ni2-O1W=0.206 5(3) and 0.207 7(3) nm; O1W-Ni2-O1W=175.34(12)°; O1W-Ni2-N/O=86.75(11)°~94.42(12)°). The pyta³⁻ ligand connects two Ni atoms to form a μ_2 -bridging mode (Scheme 1).

Interestingly, three Ni(II) atoms containing two Ni1 and one Ni2 form a linear trinuclear $[\text{Ni}_3(\text{pyta})_2]$ unit bridged by μ_2 -pyta ligand (Fig.6), which is different from the Fe-pyta chain in complex **1**. Furthermore, the bridging abpt ligands link the $[\text{Ni}_3(\text{pyta})_2]$ units (Fig.7a) to generate a 2D (4,4) layer (Fig.7b), in which the $[\text{Ni}_3(\text{pyta})_2]$ units act as the 4-connected nodes and abpt as the spacers. The lattice water molecules are located

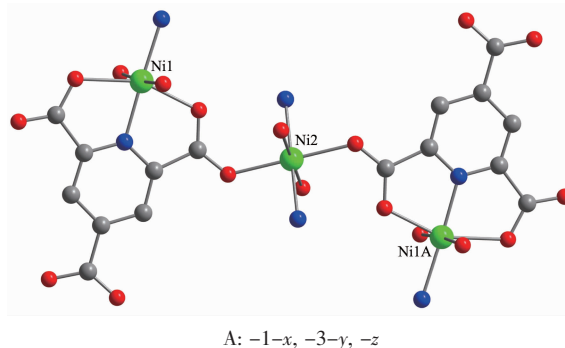


Fig.6 Linear trinuclear units $[\text{Ni}_3(\text{pyta})_2]$ bridged by pyta³⁻ ligand in **2**

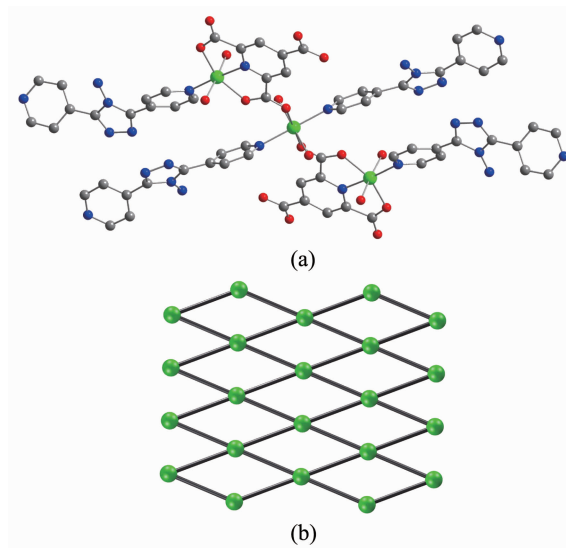


Fig.7 4-connected $[\text{Ni}_3(\text{pyta})_2]$ node (a) and (4,4) topological coordination layer (b) in **2**

in the space between two layers with rich hydrogen bonds ($O \cdots O = 0.267\,9(4) \sim 0.299\,2(6)$ nm, $O-H \cdots O = 154(3)^\circ \sim 175(4)^\circ$). The 2D layers are linked to a 3D supramolecular through weak π - π interactions and hydrogen-bonds (Fig.8).

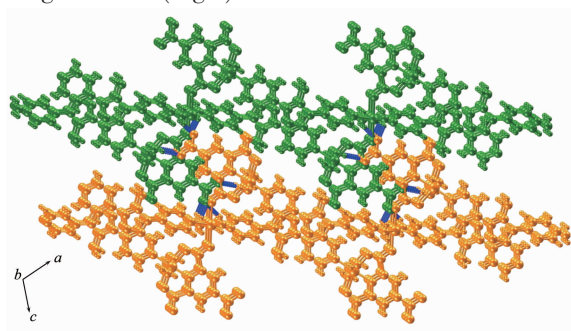


Fig.8 Perspective view of the 2D coordination layer packed to 3D supramolecular network through weak π - π interactions and hydrogen-bonds in 2

References:

- [1] Evans O R, Lin W B. *Acc. Chem. Res.*, **2002**,**35**:511~522
- [2] Yaghi O M, Li G, Li H. *Nature*, **1995**,**378**:703~706
- [3] Conn M M, Rebek J Jr. *Chem. Rev.*, **1997**,**97**:1647~1668
- [4] Zaman M B, Smith M D, Zurloye H C. *Chem. Commun.*, **2001**: 2256~2257
- [5] Kitaura R, Seki K, Akiyama G, et al. *Angew. Chem., Int. Ed.*, **2003**,**42**:428~431
- [6] Finn R C, Lam R, Greedan J E, et al. *Inorg. Chem.*, **2001**,**40**: 3745~3754
- [7] Lu J Y. *Coord. Chem. Rev.*, **2003**,**246**:327~347
- [8] Tong M L, Chen X M, Batten S R. *J. Am. Chem. Soc.*, **2003**, **125**:16170~16171
- [9] Gao H L, Yi L, Ding B, et al. *Inorg. Chem.*, **2006**,**45**:481~483
- [10] Yigit M V, Biyikli K, Moulton B, et al. *Cryst. Growth Des.*, **2006**,**6**:63~69
- [11] Li C J, Peng M X, Tong M L, et al. *Chem. Commun.*, **2008**,**47**: 6348~6350
- [12] Li C J, Peng M X, Tong M L, et al. *Cryst. Comm. Eng.*, **2008**, **10**:1645~1652
- [13] Du M, Jiang X J, Zhao X J. *Chem. Commun.*, **2005**:5521~ 5523
- [14] Dong Y B, Wang H Y, Ma J P, et al. *Cryst. Growth Des.*, **2005**,**5**:789~800
- [15] Du M, Jiang X J, Zhao X J. *Inorg. Chem.*, **2006**,**45**:3998~ 4006
- [16] Chen Z Y, Peng M X. *Chem. Res. Chinese Universities*, **2008**,**24**:392~395
- [17] CHEN Zi-Yun(陈梓云), PENG Meng-Xia(彭梦侠). *Chinese J. Inorg. Chem.(Wuji Huaxue Xuebao)*, **2007**,**23**:2091~2096
- [18] Syper L, Kloc K, Mlochowski J. *Tetrahedron*, **1980**,**36**:123~ 129
- [19] Fouad B, Michel L, Michel T, et al. *J. Heterocyclic Chem.*, **1999**,**36**:146~149
- [20] Sheldrick G M. *SADABS 2.05*, University of Göttingen
- [21] *SHELXTL 6.10*, Bruker Analytical Instrumentation, Madison, Wisconsin, USA, **2000**.
- [22] Wang J, Lin Z J, Tong M L, et al. *Chem. Eur. J.*, **2008**,**14**: 7218~7235